SIMULATION OF SEMICONDUCTOR DEVICES AND PROCESSES Vol. 4
Edited by W. Fichtner, D. Aemmer - Zurich (Switzerland) September 12-14, 1991 - Hartung-Gorre

A new microscopic model for hole transport in silicon with application to sub-micron LDD MOSFETs

A. Abramo, C. Fiegna, F. Venturi†, R. Brunetti‡, E. Sangiorgi, C. Bergonzoni°, and B. Riccò

DEIS, University of Bologna, v.le Risorgimento 2, 40136 Bologna, Italy

† *Dept. of Information Engineering, University of Parma, Italy*
‡ *Dept. of Physics, University of Modena, Italy*
° *SGS Thomson Central R&D Agrate B.za (Milano), Italy*

Abstract

A new microscopic silicon model for hole transport at high electric fields featuring two isotropic valence bands in a finite spherical Brillouin zone is presented. The band parameters and the electron-phonon coupling constants were determined by best fitting the hole density of states and the transport properties. Applications to LDD n-MOSFET degradation analysis are presented.

1. The band model

When electron and hole transport properties are studied at very high electric fields ($F \geq 100kV/cm$) and/or very high carrier energies ($E \geq 1eV$), traditional models, including only the lowest set of minima of the conduction band and the top of the valence band in a simple effective-mass approximation [1], are no longer adequate. Important effects like the finite dimensions of the Brillouin zone (BZ) and the non-monotonic behavior of the density of states (DOS) as a function of energy cannot be neglected in any (analytical or numerical) reliable description.

Some attempts at improving the theoretical scheme used in Monte Carlo simulations have been presented in the literature [2,3].

This work presents an original microscopic model for hole transport in silicon at high fields which extends the traditional band model to include these relevant effects, also maintaining a simple physical interpretation, and incorporates a treatment of electron-phonon interaction consistent with the band model. The simplifications introduced in this model, even though not affecting the accuracy of the description, allow to perform Monte Carlo simulations of small electronic devices with good computational efficiency.

Following the same line of the transport model for electrons described elsewhere [4] we developed an original microscopic model for holes thus allowing to simulate bipolar transport in a device, treating both types of carriers with the same level of accuracy.

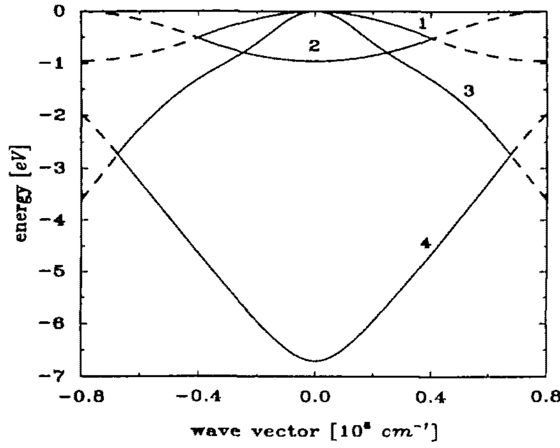

Figure 1: Band structure of present model. For simplicity, here and in the text hole energies are considered positive and relative to the top of the valence band.

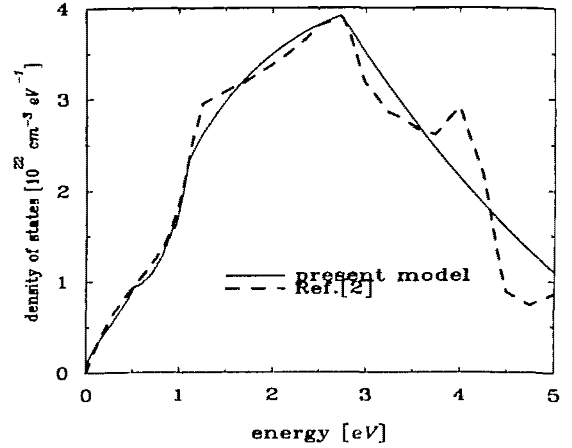

Figure 2: Comparison between valence band DOS of present model and that in Ref.[5].

The new model includes two isotropic bands in a finite spherical BZ, as shown in Fig.1, where each part, corresponding to different analytical expression, is differently labeled. These two bands provide a best fit to the DOS as a function of energy obtained from a first-principle band structure calculation [5], as shown in Fig.2.

The DOS contains integrated informations over the whole band structure and it has an essential role in the evaluation of the carrier-phonon scattering rate.

The analytical dependence $E(\mathbf{k})$ was obtained by using the well-known non parabolic approximation

$$(E - E_0)(1 + \alpha(E - E_0)) = \frac{\hbar^2(k - k_0)^2}{2m^*}$$

where in our case the parameters α, m^* and the geometrical multiplicity factor Z are not constant along the two bands, but can assume different values for different portions of the two bands, in order to account for the warping of the real band structure, but always maintaining continuity of energy, group velocity and DOS. The spherical BZ is assumed to have a finite dimension, which is different for different bands and is assumed again as a parameter.

At low energies the two bands have the traditional shape of heavy and light holes, respectively [6]; approaching the energy of $1eV$ from the top of the valence band, at which the first band terminates, and higher, the shape of the second band becomes somewhat more complex (see Fig.1). At these energies, in fact , because of the warping of the valence band, the DOS accounts for contributions of bands along different k-space directions. In the present model such contributions are taken into account by making the effective mass and the band multiplicity to increase with energy.

The values of the parameters for the analytical expressions of the bands are reported in Table 1.

Acoustic intraband and optical interband phonon scatterings have been included, with

band part	$E[eV]$	$k[10^8 cm^{-1}]$	$\alpha[eV^{-1}]$	m^*	$E_0[eV]$	$k_0[10^8 cm^{-1}]$	Z
1	$0 \leq E \leq 0.5155$	$0 \leq k \leq 0.404$	0.4	1.0	0.0	0.0	1
2	$0.5155 < E \leq 0.9558$		0.0	−1.4124	0.9558	0.0	1
3	$0 \leq E \leq 0.2$	$0 \leq k \leq 0.1259$	0.1	0.2	0.0	0.0	2
	$0.2 < E \leq 1.1$	$0.1259 < k \leq 0.3398$	0.0	−1.0736	1.7392	0.7642	$Z(E)$
	$1.1 < E \leq 2.7337$	$0.3398 < k \leq 0.675$	−0.045	0.9	0.6	0.0	6
4	$2.7337 < E \leq 6.7092$	$0 < k \leq 0.675$	0.5	−0.1462	6.7092	0.0	6

Table 1: Parameters for bands of present model. $Z(E)$ means Z varying from 2 to 6 between 0.5 and 1.0 eV. The labels refer to Fig. 1.

coupling strengths $5.78 eV$ and $6 \times 10^8 eV/cm$ respectively. These values are quite similar to those reported in literature [1,2] and were determined from a best fit of transport properties. Fig.3 reports the total phonon scattering rate as a function of energy for the two bands of Fig.1. It can be seen that the behavior of the scattering rate resembles the shape of the DOS.

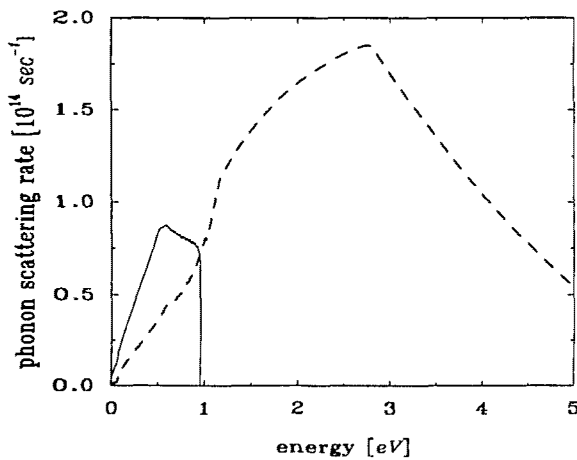

Figure 3: Phonon scattering probability for first (solid line) and second (dashed line) hole band.

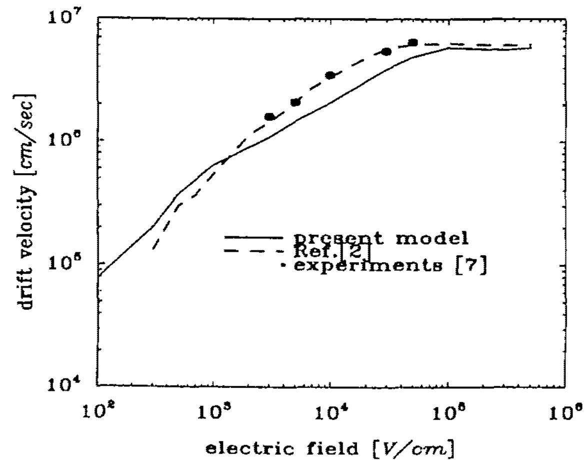

Figure 4: Hole drift velocity compared with experimental data [7] and simulations of Ref.[2].

The model has been validated by comparison with available experimental data of drift velocity in bulk silicon for the low-intermediate field range [7], and with drift velocity and mean energy obtained by advanced Monte Carlo simulations including the complete silicon band structure [2] (Figs.4,5). The agreement between mean-energy data is very good, while some discrepancies can be observed in the drift-velocity data at intermediate electric fields, which disappear at the highest fields considered. From the analysis of Figs.4,5 we can conclude that the present model provides a satisfactory modeling of hole transport.

Finally Fig.6 reports the band occupancy as a function of the electric field strength and shows the increasing importance of the light-hole band at high fields.

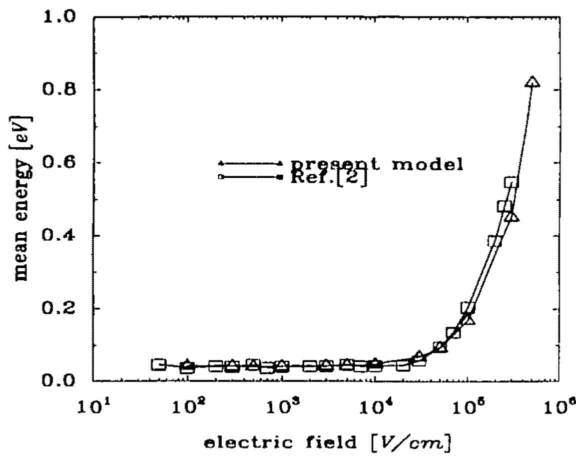

Figure 5: Hole mean energy compared with simulations in Ref.[2].

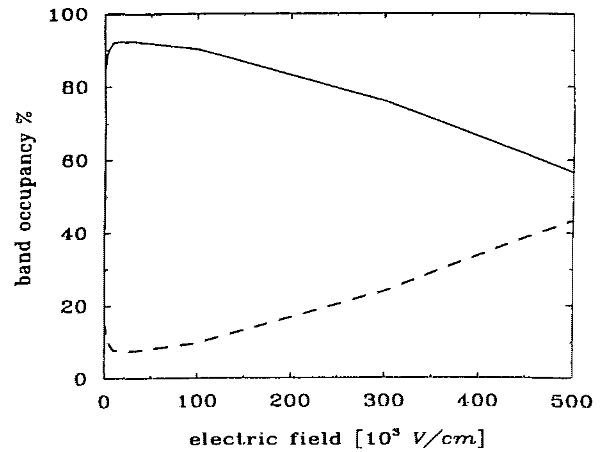

Figure 6: Population percentage for first (solid line)and second (dashed line) hole band.

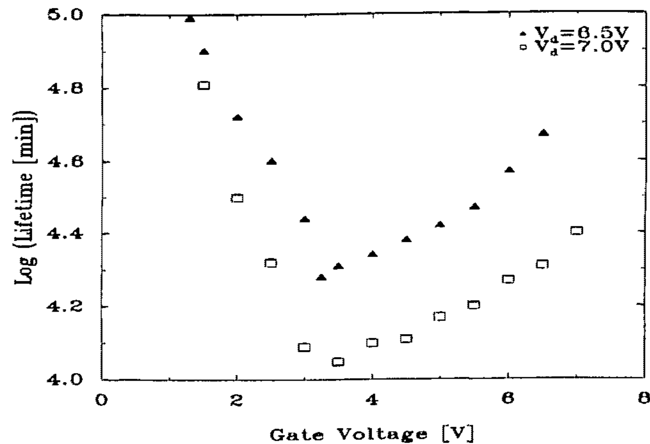

Figure 7: Extrapolated lifetime at $V_{ds} = 6.5V$ (triangle) and $V_{ds} = 7V$ (square) vs. gate bias.

2. Application to device simulation

The model described above has been included in the Monte Carlo-Poisson device simulator BEBOP [8] which features a previously developed multi-band model for electrons in Si [4] and an anisotropic impact-ionization (II) model [9]. This allowed to study the transport of II generated holes and their role, together with hot electrons, in n-MOSFET degradation. Such a problem has been extensively studied [10] but, since no agreement has been reached on the relative role played by hot electrons and holes generated by II in causing the $Si - SiO_2$ interface damage,

a more detailed and physically based analysis is still required. A preliminary study has been reported in [11] where a simplified model was used for hole transport. Here the use of the new hole model gives us more confidence in making comparisons with experimental data on device degradation obtained from submicrometer LDD n-MOSFETs.

DC accelerated stress tests on n-MOS transistors were performed under different bias conditions, in order to analyze the degradation intensity dependence on the specific operating mode. The studied devices were $0.8\mu m$ gate length LDD n-channel transistors, manufactured with twin-well C-MOS process, featuring $21nm$ dry gate oxide thickness, $0.3\mu m$ sidewall oxide spacers and N^+ polysilicon/tungsten silicide stacked gate electrode. The effective channel length was estimated to be about $0.5\mu m$ from electrical measurements.
As a monitor of the hot carrier induced degradation, the drain current in the linear region ($V_d = 0.1V$, $V_g = 5V$) was measured at fixed time intervals. The measured results were extrapolated to 10% current degradation to extract the device lifetime, following a power law model for the chosen parameter degradation [12]. The measurements were performed at $V_d = 6.5V$ and $V_d = 7.0V$ at several gate voltage V_g. Each of the experimental points come from averaging over three samples, in order to reduce the impact on the results of eventual gate length fluctuations. Fig. 7 shows the extrapolated lifetimes for the stress conditions defined above. The dependence of the lifetime on the gate voltage shows the typical minimum at $V_g = V_d/2$, corresponding to the maximum substrate current. This bias condition has been widely reported to induce the maximum interface state generation.

The unstressed devices have been simulated in the three relevant conditions: $V_{gs} = V_{ds}/5 = 1.4V$, $V_{gs} = V_{ds}/2 = 3.5V$ and $V_{gs} = V_{ds} = 7V$. Some results concerning electron and hole heating at the $Si - SiO_2$ interface are summarized in Figs.8-11. The simulation results are not directly related to the degradation data of Fig.7 because the electron/hole trapping process and its effect on the device drive capability has not been included in the simulation. However they can be helpful in determine the role of the two carriers in the degradation process.

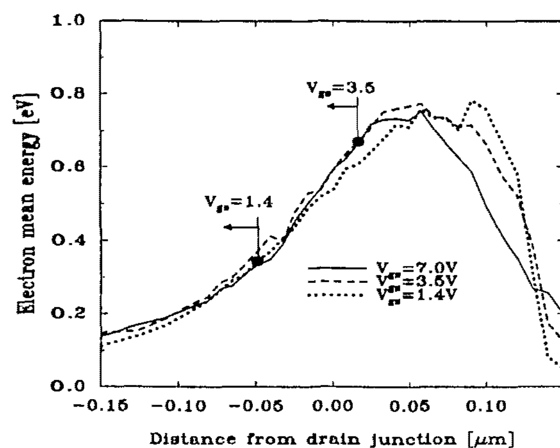

Figure 8: Hole mean energy at the interface. Arrows indicate the region where oxide field is attractive.

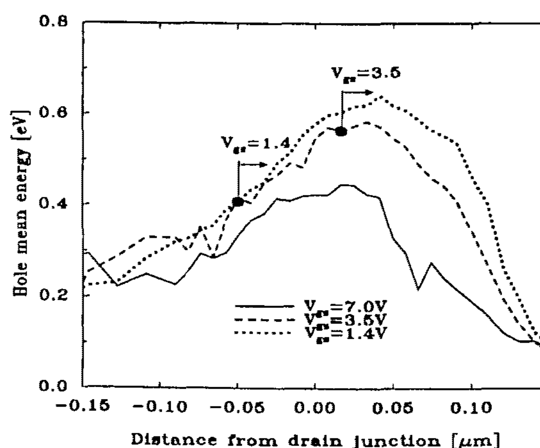

Figure 9: Hole mean energy at the interface. Arrows indicate the region where oxide field is attractive.

Fig.8(9) shows the electron (hole) mean energy at the surface in the vicinity of the drain junction for the three different bias conditions. The bullets indicate the position in the channel where the vertical field vanishes for the conditions $V_{gs} = 1.4V$ and and $V_{gs} = 3.5V$, i.e. the oxide field is attractive for the electrons on the left of the bullets and repulsive on the right. The opposite holds for holes. For the third condition ($V_{gs} = 7V$) the field is always attractive for electrons and repulsive for holes.

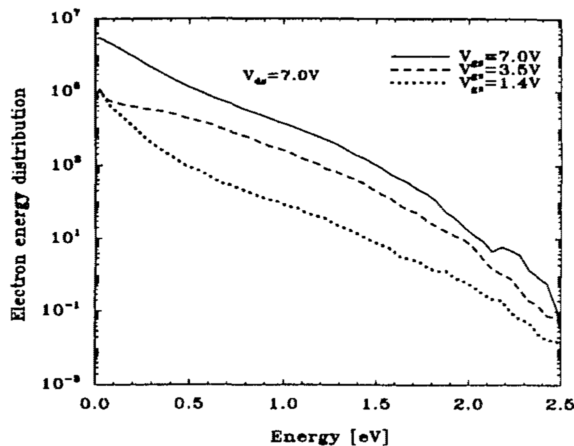

Figure 10: Electron energy distribution integrated over the high field region of MOSFET interface

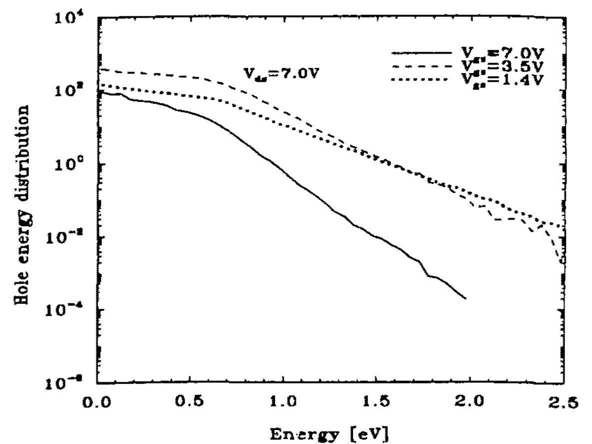

Figure 11: Hole energy distribution integrated over the high field region of MOSFET interface

Fig.10(11), instead, shows the electron (hole) energy distribution integrated over the portion of the MOSFET surface considered in the previous two figures. In addition each curve has been normalized so that its integral is proportional to the carrier population in the considered region.

From Fig.8 it can be seen that the peak of electron mean energy seems not to depend on gate bias, but the oxide field distribution makes hot-electron injection more favorable at increasing V_{gs} as the region of attractive field increases and gradually covers the device areas in the drain vicinity where the electron mean energy is higher. Fig.9 shows that hole mean energy is a decreasing function of gate bias and that, opposite to the electron case, the oxide field becomes more and more favorable to hole injection as V_{gs} is decreased.

A different perspective is given by the next two figures reporting a quantitative information on the number of hot carriers that are present at the surface in the vicinity of the drain junction in the three different bias conditions. Fig.10 shows that hot-electron population (e.g. $E > 2eV$) decreases with decreasing V_{gs} mainly due to a reduction in electron concentration. As for holes, Fig.11 suggests that hot holes are comparable in number in the two conditions $V_{gs} = 3.5V$ and $V_{gs} = 1.4V$ while are sharply decreased as the gate is raised to $7.0V$.

Therefore at $V_{gs} = 1.4V$ the number of hot electrons at the surface is minimum (Fig.10) and in addition they are subjected to a repulsive oxide field (Fig.8). Conversely, at $V_{gs} = 7V$, very few hot holes are present at the surface (Fig.11) and furthermore they are pushed away by repulsive oxide field.

From the comparison of experimental and simulation results a qualitative physical scenario

for LDD n-MOSFET degradation can be drawn. The minimum of lifetime occurring at $V_{gs} = 3.5V$ well correlates to a situation in which both hot electrons and hot holes are present at the surface and pushed towards it by the field, possibly being injected into SiO_2 or, anyway, damaging it. This correlation indicates that the most efficient degradation mechanism requires the joint action of electrons and holes. A maximum lifetime for $V_{gs} = 1.4V$, a condition in which several hot holes and few hot electrons are present, seems to rule out a degradation mechanism requiring the presence of hot holes only. Finally, at $V_{gs} = 7.0V$, in the absence of hot holes, an intermediate value for lifetime is found, suggesting the existence of a degradation mechanism that requires the presence of hot electrons only.

REFERENCES

[1] C. Jacoboni et al. *Rev. Mod. Phys.* **55**, 645, (1983).

[2] M. Fischetti et al. *IEEE Trans. Elec. Dev.* **38**, 634, (1991).

[3] N. Sano et al. *Appl. Phys. Lett.* **55**, 1418, (1989).

[4] R. Brunetti et al. *Solid-State Electronics* **12**, 1663, (1989).

[5] J.R. Chelikowsky et al. *Phys. Rev. B* **14**, 556, (1976).

[6] C. Jacoboni et al. *Advances in Physics* **28**, 493, (1979).

[7] L. Ottaviani et al. *Phys. Rev. B* **12** 3318, (1975).

[8] F. Venturi et al., *IEDM Tech. Dig.*, 485, (1989).

[9] R.Thoma et al. *J. Appl. Phys.* **69**, 2300, (1991).

[10] C. Hu et al., *IEEE Trans. Elec. Dev.* **32**, 375, (1985).

[11] F. Venturi et al., *IEDM Tech. Dig.* 455, (1990).

[12] E. Takeda et al., *IEEE Elec. Dev. Lett.* 111, (1983).